Journal of Organometallic Chemistry 694 (2009) 1998–2004

Contents lists available at ScienceDirect

Journal of Organometallic Chemistry

journal homepage: www.elsevier.com/locate/jorganchem

Synthesis, characterization and DNA binding studies of penta- and hexa-coordinated diorganotin(IV) 4-(4-nitrophenyl)piperazine-1-carbodithioates

Zia-ur-Rehman [a], Afzal Shah [a], Niaz Muhammad [a], Saqib Ali [a,*], Rumana Qureshi [a], Ian Sydney Butler [b]

[a] Department of Chemistry, Quaid-i-Azam University, Islamabad 45320, Pakistan
[b] Department of Chemistry, McGill University, 801 Sherbrook St. West, Montreal, Quebec, Canada H3A2K6

ARTICLE INFO

Article history:
Received 28 November 2008
Received in revised form 15 January 2009
Accepted 27 January 2009
Available online 5 February 2009

Keywords:
Dithiocarboxylate
Diorganotin(IV) complexes
Spectroscopy
Complex–DNA interaction

ABSTRACT

Two chlorodiorganotin(IV) complexes with general formula R_2SnClL (R = *n*-C_4H_9 **(1)** and C_2H_5 **(2)** and a diphenyltin(IV) derivative with general formula Ph_2SnL_2 **(3)**, where L = 4-(4-nitrophenyl)piperazine-1-carbodithioate ligand, were prepared and characterized by elemental analysis, Raman, FT-IR, multinuclear NMR (^1H, ^{13}C and ^{119}Sn) and mass spectrometry. On the basis of spectroscopic data the effective coordination number of Sn atom was found five (**1** and **2**) and six (**3**) both in solution and solid state. Electrochemical, kinetic and thermodynamic parameters of complexes **1–3**, interacting with DNA were evaluated by cyclic voltammetry. The linearity of the plots between the peak current (I) and the square root of the scan rate ($v^{1/2}$) indicated the electrochemical processes to be diffusion controlled. The diffusion coefficients of the free (D_f) and DNA bound forms (D_b), standard rate constants (ks) and charge transfer coefficients (α) were determined by the application of Randle–Sevcik, Nicholson and Kochi equations. The values of binding constant and binding site size were evaluated from voltammetric data. The results revealed the following increasing order of binding strength: **1** (5.4×10^3) < **3** (8.4×10^3) < **2** (1.24×10^4) M^{-1}. The UV–Vis spectroscopic data also indicated the same order of binding strength. Furthermore, the binding mode was suggested on the base of shift in peak potential (CV) and absorption maxima (UV–Vis spectroscopy).

1. Introduction

Cancer is a leading cause of premature death in the world. It can be cured by preventing the rapid proliferation of cancer cells for which the replication of DNA is to be arrested. Such an objective can be achieved either by (i) ionizing radiation via reactive oxygen species or (ii) chemotherapy using chemical substances that directly interact with DNA. Metallocomplexes of platinium(II) like cisplatin, oxalylplatin, nedaplatin and carboplatin achieved clinical status as a result of intensive research focused on anti-cancer coordination compounds. However, in spite of their high activity, the applications of cisplatin and similar compounds are limited by serious disadvantages like: (a) poor water solubility (b) toxicity and (c) tolerance by the tumor. In the search for effective alternatives, Organotin(IV) dithiocarboxylates received utmost attention on account of their potential apoptotic inducing character. Moreover, these complexes have limited side effects with high therapeutic index as compared to the clinically used cisplatin and carboplatin [1].

Deoxyribonucleic acid (DNA) plays an essential role in biological processes since it is the storehouse of genetic information. Various mutagens can damage its replication machinery which may lead to programmed cell death. The proliferation of cancer cells can be prevented by the interaction of DNA binding molecules which may dysfunction it either by strand scission or chain cutting or local unwinding of its double helical structure, leading to various pathological changes in living organisms.

The investigation of drug–DNA interaction is important for understanding the molecular mechanism of drug action and designing [2]. Such interactions are studied by a variety of techniques like cyclic voltammetry, UV–Vis, fluorescence, Raman and NMR spectroscopy [3]. The interaction of some metal chelates of Co(III), Ru(II) and Os(II) with DNA were studied by cyclic voltammetry [4–7] but their lower affinity to DNA prompted the researchers to concentrate their efforts on other potential metal complexes. In the quest for exploring effective DNA binders and as per our interest in organotin(IV) dithiocarboxylates [8–10], we synthesized three potential anti-cancer tin based chelates of 4-(4-nitrophenyl)piperazine-1-carbodithioate, characterized and investigated their interaction with DNA by cyclic voltammetry and UV–Vis spectroscopy. The structure of ligand-salt and organic groups attached to Sn atom along with numbering scheme is presented in Scheme 1.

* Corresponding author.
E-mail address: drsa54@yahoo.com (S. Ali).

0022-328X/$ - see front matter © 2009 Elsevier B.V. All rights reserved.
doi:10.1016/j.jorganchem.2009.01.047

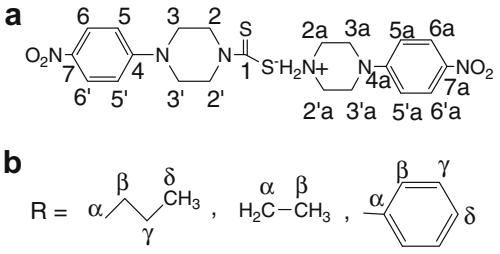

Scheme 1.

2. Experimental

2.1. Materials and methods

Reagents, *n*-Bu_2SnCl_2, Et_2SnCl_2 Ph_2SnCl_2 and 4-(4-nitrophenyl) piperazine were obtained from Aldrich, dimethylsulphoxide (DMSO) with 99.5% purity and CS_2 from Riedal-de-Haën; methanol from E. Merck was dried before use by the reported method [11]. DNA was extracted from human blood by Falcon method [12]. The purity of DNA was checked from the ratio of absorbance at 260 and 280 nm (A_{260}/A_{280} = 1.85). The concentration of the stock solution of DNA (2.5 mM in nucleotide phosphate, NP) was determined by monitoring the absorbance at 260 nm, using the molar extinction coefficient (ε) of 6600 M^{-1} cm^{-1}. Electrochemical grade tetrabutylammonium fluoroborate (TBAFB) purchased from Fluka was used as supporting electrolyte. Nitrogen saturated solutions were obtained by bubbling high purity N_2 for at least 10 min in the solution and keeping the environment of the pure gas over the solution during the voltammetric experiments.

Microanalysis was done using a Leco CHNS 932 apparatus. Raman spectra (±cm^{-1}) were measured with an InVia Renishaw spectrometer, using argon-ion (514.5 nm) and near-infrared diode (785 nm) lasers. WIRE 2.0 software was used for the data acquisition and spectra manipulations. IR spectra in the range 4000–400 cm^{-1} were obtained on bio-Rad FT-IR spectrophotometer with samples investigated as KBr discs or thin film on NaCl cell. NMR spectra (d_6-DMSO) were obtained using Hg-300 and a Varian Unity 500-MHZ instruments. Electron impact (70 eV) mass spectra were recorded on a Kratos MS25RFA instrument. Electrochemical experiments were carried out using an Autolab PGSTAT 302 running with GPES (General Purpose Electrochemical System) version 4.9, software (Eco-Chemie, Utrecht, The Netherlands). Voltammograms were recorded at room temperature using a three-electrode system; a glassy carbon-electrode of 0.071 cm^2 area as working electrode, a saturated calomel electrode (SCE) as a reference and platinum wire as counter electrode. Prior to every electrochemical assay, the working electrode was used to polish with 0.25-μm diamond paste on a nylon buffing pad, followed by washing with water. All the experiments were carried out at room temperature (ca. 25 ± 1 °C).

2.2. Synthesis

2.2.1. Synthesis of 4-(4-nitrophenyl)piperazinium 4-(4-nitrophenyl)piperazine-1-carbodithioate (L-salt)

Dropwise addition of CS_2 (in excess) in methanol (50 mL) to 4-(4-nitrophenyl) piperazine (5 g, 24.15 mmol) in methanol (50 mL) followed by stirring for 4 h at 0 °C gave the yellowish product. The yellow product was filtered off and was washed with diethyl ether (Yield: 4.91 g, 83%). M.p. 180–182 °C. Elemental Anal. Calc. for $C_{21}H_{26}N_6O_4S_2$: C, 51.41; H, 5.34; N, 17.13; S, 13.07. Found: C, 51.37; H, 5.30; N, 17. 11; S, 13.01%. Raman (cm^{-1}): 664 ν(C–S), 1210 ν(C═S), 1507 ν(C–N). IR (cm^{-1}): 1030 ν(C–S), 1478 ν(C–N). ^{1}H NMR (ppm): 8.1, 8.0 (d, $H_{6,6',6a,6'a}$, $^3J_{H-H}$ = 9.6 Hz), 7.1, 6.9 (d, $H_{5,5',5a,5'a}$ $^3J_{H-H}$ = 9.6 Hz). 4.42–4.39, 3.69–3.65 (m, $H_{3,3',3a,3'a}$). 3.50–3.47, 3.27–3.24 (m, $H_{2,2',2a,2'a}$). ^{13}C NMR (ppm): 213.5 (C-1), 154.9, 154.7, 138.4, 137.1, 131.3, 126.3, 114.0, 112.6 (Ar-C). 49.0, 46.3 (C-3, 3′, 3a, 3′a), 43.1, 40.9 (C-2, 2′). EI-MS, *m*/*z* (%): $[C_{10}H_{14}N_3O_2]^{\cdot+}$ 208 (4.7), $[C_{10}H_{13}N_3O_2]^{\cdot+}$ 207 (38.7), $[C_8H_9N_2O_2]^+$ 165 (100), $[C_8H_9\ N_2O]^+$ 149 (4), $[C_8H_9N]^{\cdot+}$ 119 (19.8), $[C_6H_5]^+$ 76 (24.4).

2.2.2. Synthesis of chlorodibutylstannyl 4-(4-nitrophenyl)piperazine-1-carbodithioate (**1**)

Bu_2SnCl_2 (0.53 g, 1.76 mmol) and L-salt (0.862 g, 1.76 mmol) was mixed together in methanol (90 mL) and the mixture was refluxed for 6 h with constant stirring, the yellowish product thus obtained was filtered and recrystallized from chloroform–ethanol (Yield: 0.74 g, 77%). M.p. 115–117 °C. Elemental Anal. Calc. for $C_{19}H_{30}N_3O_2S_2SnCl$: C, 41.43; H, 5.49; N, 7.63; S, 11.64. Found: C, 41.38; H, 5.45; N, 7.57; S, 11.55%. Raman (cm^{-1}): 614 ν(C–S), 1202 ν(C═S), 1507 ν(C–N), 517 ν(Sn–C), 346 ν(Sn–S), 263 ν(Sn–Cl). IR (cm^{-1}): 1125, 1006 $\nu(CS_2)$, 1487 ν(C–N), 502 ν(Sn–C). EI-MS, *m*/*z* (%): $[C_{15}H_{21}N_3O_2S_2SnCl]^+$ 494 (2), $[C_4H_9S_2SnCl]^{\cdot+}$ 276 (6), $[C_4H_9S_2Sn]^+$ 241 (21), $[S_2SnCl]^+$ 219 (30), $[S_2Sn]^{\cdot+}$ 184 (9), $[C_4H_9Sn]^{\cdot+}$ 177 (6), $[SnCl]^{\cdot+}$ 155 (43). ^{1}H NMR (ppm): 8.08 (d, $H_{6,6'}$, $^3J_{H-H}$ = 9.3 Hz), 6.77 (d, $H_{5,5'}$, $^3J_{H-H}$ = 9.3 Hz), 4.29–4.19 (m, $H_{3,3'}$), 3.64–3.57 (m, $H_{2,2'}$), 2.08–1.35 (m, CH_2, $SnBu_2$), 0.92 (t, CH_3, $SnBu_2$, ^3J = 7.2 Hz). ^{13}C NMR (ppm): 198.5 (C-1), 154.0, 138.9, 126.2, 112.6 (C-Ar), 50.7 (C-2, 2′), 46.0 (C-3, 3′), 29.6 (C-β), 28.0 (C-γ), 26.5 (C-α), 13.9 (C-δ). ^{119}Sn NMR: δ = −185 ppm.

2.2.3. Synthesis of chlorodiethylstannyl 4-(4-nitrophenyl)piperazine-1-carbodithioate (**2**)

Compound **2** was prepared in the same way as **1**, using the same molar amounts, to give yellow crystals. (Yield: 0.63 g, 72%). M.p. 156–157 °C. Elemental Anal. Calc. for $C_{15}H_{22}N_3O_2S_2SnCl$: C, 36.42; H, 4.48; N 8.49; S, 12.96. Found: C, 36.38; H, 5.46; N, 8.43; S, 12.87%. Raman (cm^{-1}): 615 ν(C–S), 1202 ν(C═S), 1511 ν(C–N), 513 ν(Sn–C), 350 ν(Sn–S), 268 ν(Sn–Cl). IR (cm^{-1}): 1124, 1002 $\nu(CS_2)$, 1490 ν(C–N), 503 ν(Sn-C). EI-MS, *m*/*z* (%): $[C_{13}H_{17}N_3O_2S_2SnCl]^+$ 466 (2), $[C_2H_5S_2SnCl]^{\cdot+}$ 248 (9), $[S_2SnCl]^+$ 219 (47), $[C_2H_5S_2Sn]^+$ 213 (21), $[S_2Sn]^{\cdot+}$ 184 (11), $[SnCl]^+$ 155 (51), $[C_2H_5Sn]^+$ 149 (6), $[Sn]^{\cdot+}$ 120 (10). ^{1}H NMR (ppm): 8.12 (d, $H_{6,6'}$, $^3J_{H-H}$ = 9.0), 6.81 (d, $H_{5,5'}$, $^3J_{H-H}$ = 9.0 Hz), 4.20–4.17 (m, $H_{3,3'}$), 3.65–4.12 (m, $H_{2,2'}$), 1.84 (q, CH_2, $SnEt_2$, $^3J_{H-H}$ = 6.0 Hz), 1.47 (t, CH_3, $SnEt_2$, $^3J_{H-H}$ = 6.0). ^{13}C NMR (ppm): 197.0 (C-1), 153.7, 139.0, 126.2, 112.6 (C-Ar), 50.7 (C-2, 2′), 46.0 (C-3, 3′), 21.6 [(C-α), $^1J^{119}$Sn–^{13}C = 530], 10.5 (C-β). ^{119}Sn NMR: δ = −177.

2.2.4. Synthesis of diphenylstannyl bis[4-(4-nitrophenyl)piperazine-1-carbodithioate] (**3**)

Compound **3** was prepared in the same way as **1**, using the ligand-salt to Ph_2SnCl_2 ratio 2:1, to give yellow solid. (Yield: 1.08 g, 73%). M.p. 224–226 °C. Elemental Anal. Calc. for $C_{34}H_{34}N_6O_4S_4Sn$: C, 48.75; H, 4.09; N, 10.03; S, 15.31. Found: C, 48.67; H, 3.95; N, 9.97; S, 15.25%. Raman (cm^{-1}): 653 ν(C–S), 1196 ν(C═S), 1305 ν(C–N), 269 ν(Sn–C), 365 ν (Sn–S), IR (cm^{-1}): 1112, 988 $\nu(CS_2)$, 1488 ν(C–N). EI-MS, *m*/*z* (%): $[C_{34}H_{34}N_6O_4S_4Sn]^{\cdot+}$ 838 (0.4), $[C_{22}H_{26}N_4OS_4Sn]^+$ 610 (1.7), $[C_{16}H_{21}N_4OS_4Sn]^{\cdot+}$ 533 (12), $[C_{16}H_{21}N_4\ OS_3\ Sn]^+$ 501 (8), $[C_{12}H_{13}N_2OS_3Sn]^{\cdot+}$ 417 (3), $[C_6H_5Sn]^+$ 197 (39), $[Sn]^{\cdot+}$ 120 (19). ^{1}H NMR (ppm): 8.06 (d, $H_{6,6'}$, $^3J_{H-H}$ = 9.3 Hz), 6.91 (d, $H_{5,5'}$, $^3J_{H-H}$ = 9.3), 4.13–4.06 (m, $H_{3,3'}$), 3.72–3.69 (m, $H_{2,2'}$), 7.94 (bs, H_o, $SnPh_2$), 7.46 (bs, $H_{m,p}$, $SnPh_2$). ^{13}C NMR (ppm): 197.5 (C-1), 154.2, 137.7, 126.4, 112.8 (C-Ar), 51.8 (C-2, 2′), 45.1 (C-3, 3′), 135.7 (C-α), 131.3 (C-β), 130.1 (C-γ), 129.5 (C-δ). ^{119}Sn NMR: δ = −333.

3. Results and discussion

3.1. Proposed mechanism of ligand and complexes **1–3** synthesis

The nucleophilic attack of 4-(4-nitrophenyl)piperazine on carbon disulfide gave as 4-(4-nitrophenyl)piperazine-1-carbodithioic acid as intermediate which undergoes acid–base reaction with unreacted 4-(4-nitrophenyl)piperazine to gave 4-(4-nitrophenyl) piperazinium 4-(4-nitrophenyl)piperazine-1-carbodithioate (L-salt). The reaction of the equimolar ligand-salt with R_2SnCl_2 (R = Bu, Et) gave R_2SnLCl and 4-(4-nitrophenyl)piperazinium chloride while refluxing Ph_2SnCl_2 with ligand-salt in the ratio of 1:2 gave Ph_2SnL_2 and the same by-product as shown in Scheme 2. This mechanism has been proposed on the basis of multinuclear NMR (^1H and ^{13}C) study of ligand.

3.2. Vibration spectra

The assignment of Raman bands of the three complexes has been made by comparison with the Raman spectra of their related precursors. A new absorption band at 346–365 cm^{-1} for **1–3**, which is absent from the spectra of the free ligand, can be assigned to the Sn–S stretching mode of vibration. Very sharp Sn–C peak was observed at 517 cm^{-1} in first two complexes, whereas in diphenyltin(IV) derivative a weak vibration mode at 269 cm^{-1} was assigned to Sn–C. In addition, Raman spectra of complex **1** and **2** display peaks associated with ν(Sn–Cl).

In IR spectra of organotin(IV) dithiocarboxylates, out of all the vibration modes C–N, CS_2 stretching frequencies are of particular interest in term of coordination mode of 1,1-dithioate moiety. In the IR spectra of complexes **1–3**, the strong peaks that appear at 1125–1112 cm^{-1} have been attributed to the asymmetric absorption of $\nu(CS_2)_{as}$ and the 998–1006 cm^{-1} can be assigned to the symmetric $\nu(CS_2)_s$ absorption frequencies. According to the literature [13], for complexes **1–3**, the difference of $\nu(CS_2)_{as}$ and $\nu(CS_2)_s$ are 119–124 cm^{-1}, indicating that 1,1-dithioate moiety of the ligand is linked to the central tin in a bidentate fashion. The stretching vibration peaks of the C–N, were located at ~1490 cm^{-1} and are intermediate between the values for C–N single bond (1250–1360 cm^{-1}) and C=N double bond (1640–1690 cm^{-1}). Partial double bond character for the C–N bond would result in some partial double bond character for the C–S bonds. The appearance of new peaks at ~502 cm^{-1}, in compounds **1** and **2**, were assigned to Sn–C. The analyses are in agreement with X-ray single crystal diffraction results, recently reported by our group [14,15], for complexes **1** and **2**.

3.3. NMR spectra

In the ^1H NMR spectra of the complexes, the integral ratio of the signals resulting from protons of the ligand to those from protons of the organic groups on the Sn provides a reliable measure of the metal to ligand ratio in the synthesized complexes. The disappearance of duplication peak pattern due to 4-(4-nitrophenyl)piperazinium ion and appearance of proton signals for the organic groups attached to Sn confirmed the formation of complexes **1–3**. The protons of piperazine moiety of the ligand showed two multiplet in the aliphatic region while aromatic part of the ligand gave two doublets due to two non-equivalent sets of protons in all three complexes. Dibutyl, diethyl and diphenyl groups of the organotin moiety display signals in their expected regions.

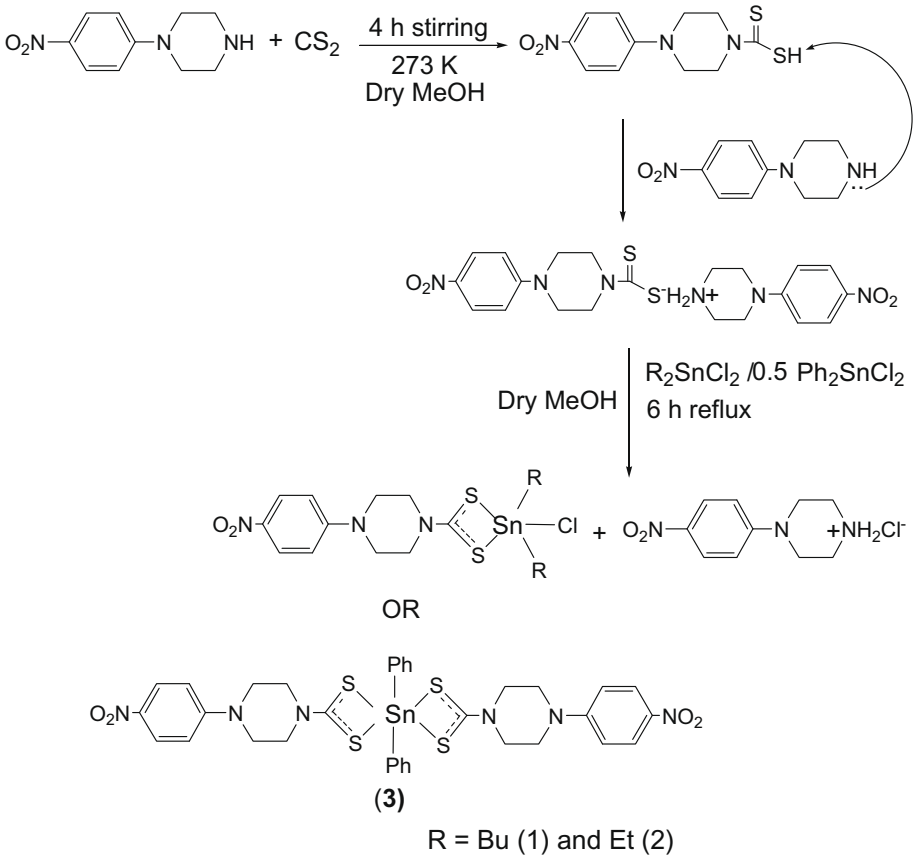

Scheme 2.

In ^{13}C NMR spectra, the duplicate peak pattern due to 4-(4-nitrophenyl)piperazinium ion disappeared due to detachment of this group from the ligand upon its complexation to Sn. A small shift in the position of C(1) was noted which resulted from deshielding of this particular carbon due to disconnection of cationic part of ligand and coordination of CS_2 moiety through both sulfur atoms to Sn. Moreover, the $^1J[^{119}Sn,^{13}C]$ coupling constant observed for complex **2**, 530 Hz, was the same as that reported for analogous 5-coordinate derivatives [16,17].

^{1119}Sn NMR spectroscopy has been found to be very useful for the elucidation of the nature of coordination in the organotin(IV) dithiocarboxylates. Even though for each complex with the same coordination number, some wide range of $\delta(^{119}Sn)$ values are observed depending on the different organic and dithiocarboxylate groups attached to the Sn atom, there is an approximate linear relationship between the ^{119}Sn values and the coordination numbers of the complexes. Thus, for the known organotin(IV) dithiocarboxylates [18], $\delta(^{119}Sn)$ have been found to lie between −150 to −250 ppm in penta-coordinate, while a range −300 to −500 ppm have been observed for hexa-coordinate Sn atom. Based on $\delta(^{119}Sn)$ value, complexes **1** and **2** showed penta-coordinate geometry while the Sn atom is six coordinate (−333 ppm) in complex **3**.

3.4. Mass spectra

Mass-spectral data for **1–3** showed rich ion distributions but our interest lies in Sn containing ions. These ions were quantitatively identified by inspection from the characteristic isotopic peak pattern for Sn [19]. The mass spectral data reported here are related to the principal isotope ^{120}Sn. Complexes **1–3** showed no molecular ion ($M^{\cdot+}$) as is generally the case for main group organometallic compounds, however, for compounds **1–3**, the different fragments observed are consistent with structures proposed on the basis of other spectroscopic techniques.

3.5. Cyclic voltammetry

The redox behavior of complexes **1–3** on clean glassy carbon-electrode was investigated in the absence and presence of DNA, using 10% aqueous DMSO at 25 °C. The CV of all the complexes (with and without DNA) showed a pair of redox waves with electrochemical parameters reported in Table 1. Typical CV behavior of **1**, in the absence and presence of DNA is shown in Fig. 1. The voltammogram of the free complex **1** shows cathodic peak at $E_{pc} = -1.308$ V, due to the reduction of **1.** On scanning in the positive direction, an oxidation peak is observed at $E_{pa} = -1.174$ V. This peak is presumably due to the oxidation of the reduction product of **1**. The difference of anodic and cathodic peak potential of about 134 mV and the ratio of their currents $I_{pc}/I_{pa} > 1$ designate the electrochemical process to be quasi-reversible. In the presence of 60 μM DNA, the 21.5% drop in cathodic peak current (I_{pc}) signifies

Table 1
CV data of compounds **1–3**[a,b,c].

Compound	CV data				
	E_{pa} (V)	E_{pc} (V)	ΔE_p (mV)	$E°$ (V)	I_{pc}/I_{pa}
1	−1.174	−1.308	134	−1.241	1.76
1-DNA	−1.274	−1.415	141	−1.344	2.10
2	−1.083	−1.191	108	−1.137	2.32
2-DNA	−0.947	−1.073	126	−1.01	1.80
3	−1.169	−1.271	102	−1.22	1.29
3-DNA	−1.096	−1.201	105	−1.148	1.37

[a]All potentials were measured versus SCE in 10% aqueous DMSO at 0.1 V s^{-1}.
[b]$\Delta E_p = (E_{pa} - E_{pc})$.
[c]$E° = (E_{pa} + E_{pc})/2$.

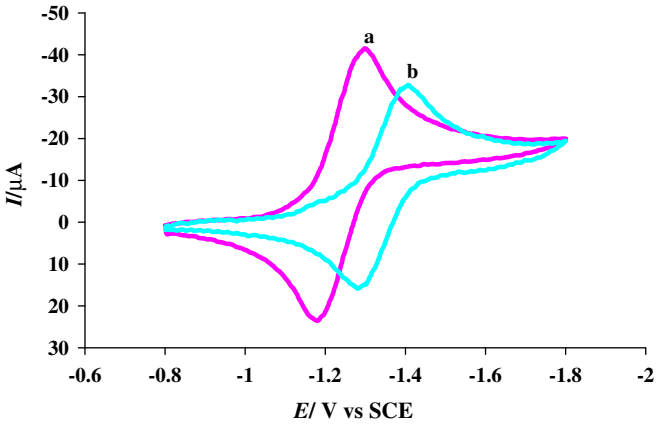

Fig. 1. CV behavior of 3 mM **1** at clean GC electrode in the absence (a) and presence of 60 μM DNA (b) in 10% aqueous DMSO using 0.1 M TBAFB as supporting electrolyte at 0.1 V s^{-1} scan rate.

the interaction of **1** with DNA. The negative shift (107 mV) in potential is ascribes electrostatic interaction of **1** with the anionic phosphate of DNA [20]. Such an interaction can be explained by the probable labile nature of dithiocarboxylate ligand due to the steric repulsion of bulky butyl groups.

The CV behavior of 3 mM **2** at 100 mV s^{-1} scan rate (Fig. 2) shows reduction at $E_{pc} = -1.191$ V and oxidation of the reduced product at $E_{pa} = -1.083$ V. In the presence of 60 μM DNA, the cathodic peak is displaced in the positive direction accompanied with the decrease in peak current. The same trend was also observed for **3.** Such peculiar CV characteristics are suggestive of intercalation of **2** and **3** into the double stranded DNA [21]. The electrochemical parameters (as obtained from CV) of complexes **1–3**, in the absence and presence of 60 μM DNA are listed in Table 1. The electron-donating groups disfavor reduction by shifting the formal potential ($E°$) in the more negative direction while the electron-withdrawing groups facilitate reduction by shifting the $E°$ to less negative values. The results reveal that the formal potential varies in the sequence: **1** > **3** > **2**, symptomatic of easy reduction of **2** due to the lower electron-donating ability of ethyl than butyl and phenyl groups. The shift of formal potentials of complexes **2** and **3** to less negative values by the addition of DNA can be attributed to their intercalation into the stacked base pairs domain of DNA. Whereas the cathodic shift of $E°$ (in case of **1**) indicates electrostatic interaction of **1** with the negatively charged oxygen of phosphate backbone of DNA.

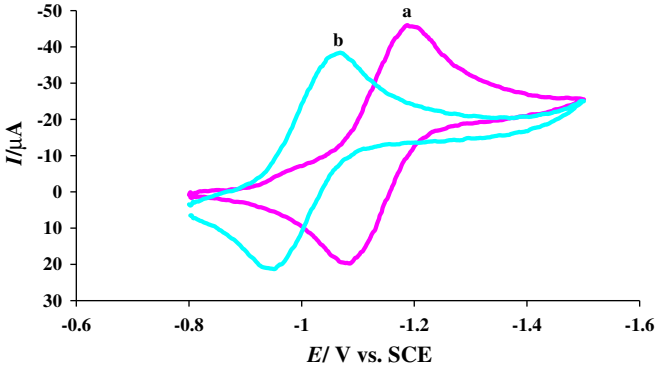

Fig. 2. CV behavior of 3 mM **2** at clean GC electrode in the absence (a) and presence of 60 μM DNA (b) in 10% aqueous DMSO using 0.1 M TBAFB as supporting electrolyte at 0.1 V s^{-1} scan rate.

The diffusion coefficients of the free and DNA bound forms of complexes **1**–**3** were determined by the application of Randle–Sevcik expression [22,23]

$$I = 2.69 \times 10^5 n^{3/2} A C_o D_o^{1/2} v^{1/2} \quad (1)$$

where I is the peak current (A), A is the surface area of the electrode (cm^2), C_o is the bulk concentration (mol cm^{-3}) of the electroactive species, D_o is the diffusion coefficient ($cm^2\ s^{-1}$), v is the scan rate ($V\ s^{-1}$) and n is the number of electrons involved in the electron transfer reaction.

The linearity of I versus $v^{1/2}$ plots (Fig. 3a and b) demonstrates, that the main mass transport of these complexes (in the absence and presence of DNA) to the electrode surface is diffusion controlled. The values of the diffusion coefficient (D_f) listed in Table 2 vary in the order: **3** > **1** > **2**, indicating greater D_f of **3**, due to the absence of chloro group which can interact strongly with the solvent, thus causing lowering of the diffusion coefficient in case of **1** and **2**. The higher D_f value of **2** as compared **1** may be due to more hydrophobic butyl than ethyl groups. The variation of molecular weights in the same order in which the D_f varies disprove the idea that a heavy molecule diffuses slowly to the electrode surface. The results reveal that the nature of the groups attached to the central metal ion plays a dominant role in deciding the order in which the values of D_f change. The D_b values of the DNA bound complexes, summarized in Table 2, are an order of magnitude smaller than the D_f values of the free complexes. The reason could be the slow mobility of the heavy complex–DNA adducts.

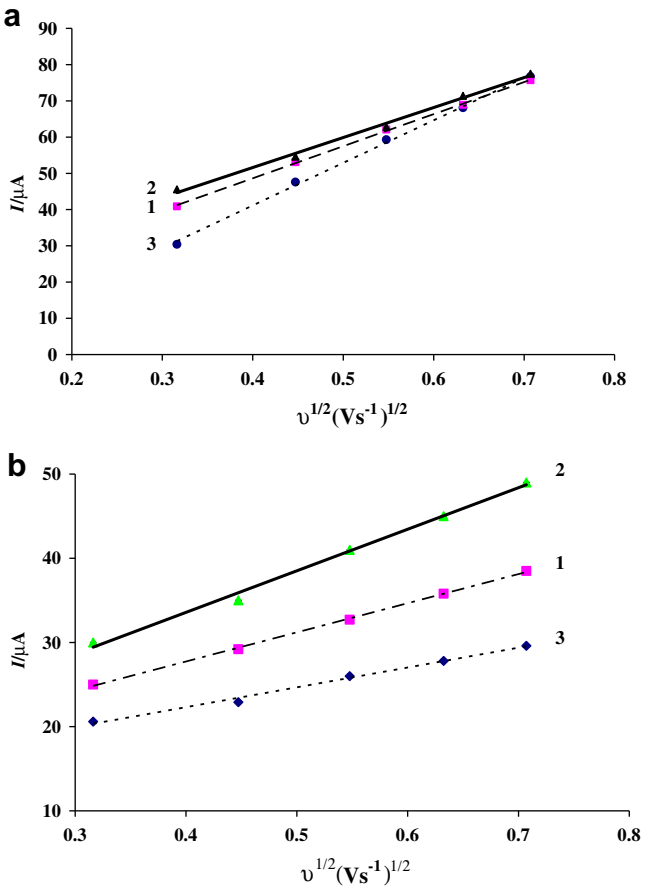

Fig. 3. (a) Plots of I vs. $v^{1/2}$, for the determination of the diffusion coefficients of 3 mM **1**–**3**. Scan rates: 0.1, 0.2, 0.3, 0.4 and 0.5 V s^{-1}. (b) Plots of I vs. $v^{1/2}$, for the determination of the diffusion coefficients of 3 mM **1**–**3** in the presence of 60 μM DNA. Scan rates: 0.1, 0.2, 0.3, 0.4 and 0.5 V s^{-1}.

The values of standard rate constant (ks) of the electron transfer reaction of these complexes at the electrode surface were obtained from Nicholson equation [24]

$$\psi = \frac{ks}{\left[\pi D_o \frac{nfv}{RT}\right]^{1/2}} \quad (2)$$

where ψ is a dimensionless parameter (depending upon peak separation, ΔE_p) and all other parameters have their usual significance.

An examination of Table 2 reflects that the ks values of DNA bound complexes are lower as compared to the free complexes. The magnitude of ks with an order of 10^{-4} corresponds to the quasi-reversible nature of the redox processes with slow electron transfer kinetics. The sequence (**3** > **2** > **1**) of the ks values without DNA, is pinpointing the fact, that the fast diffusing **3** with no chloro group is more favorable for electron transfer than complexes **1** and **2**. The slow electron transfer of **1** than **2** may be due to its greater molecular weight. For getting further evidences about the nature of the electrochemical processes of the free and DNA bound complexes **1**–**3**, the charge transfer coefficients (α) were determined by the application of Kochi formula [25]

$$\alpha = \left[\frac{(E_{1/2} - E_p^c)}{(E_p^a - E_p^c)}\right] \quad (3)$$

α with values of more than 0.5 (Table 2) for all the complexes (with and without DNA) unambiguously symbolize the quasi-reversibility of the electrochemical processes.

The sequential drop in the peak current of the complexes by the addition of increasing concentration of DNA, ranging from 20 to 60 μM, can be used to quantify the binding constant by using the equation [26] given below

$$\log(1/[\mathrm{DNA}]) = \log K + \log(I_{H-G}/(I_G - I_{H-G})) \quad (4)$$

where K is the binding constant, I_G and I_{H-G} are the peak currents of the free guest (G) and the complex (H–G), respectively.

The intercept of log (1/[DNA]) versus $\log(I_{H-G}/(I_G - I_{H-G}))$ plots (Fig. 4) yielded the binding constant K, varying in the sequence: **2**-DNA > **3**-DNA > **1**-DNA. The binding of these complexes with DNA will damage the genetic machinery resulting in the failure of the cancerous cells to replicate.

Table 2
Summary of kinetic and binding parameters of compounds **1**–**3**, as obtained from electrochemical measurements.

Compound	Kinetic parameters				Binding parameters		
	$D_f \times 10^7$ (cm^2/s)	$D_b \times 10^8$ (cm^2/s)	α	$k_s \times 10^4$ (cm/s)	s(bp)	$K \times 10^{-4}$ (M^{-1})	ΔG (kJ mol^{-1})
1	2.98	×	0.69	2.31		×	×
1-DNA	×	4.57	0.67	0.82	0.42	0.54	−21.29
2	2.61	×	0.74	3.59		×	×
2-DNA	×	9.28	0.69	1.51	0.5	1.24	−23.35
3	5.25	×	0.68	6.09		×	×
3-DNA	×	2.12	0.57	1.13	0.45	0.84	−22.39

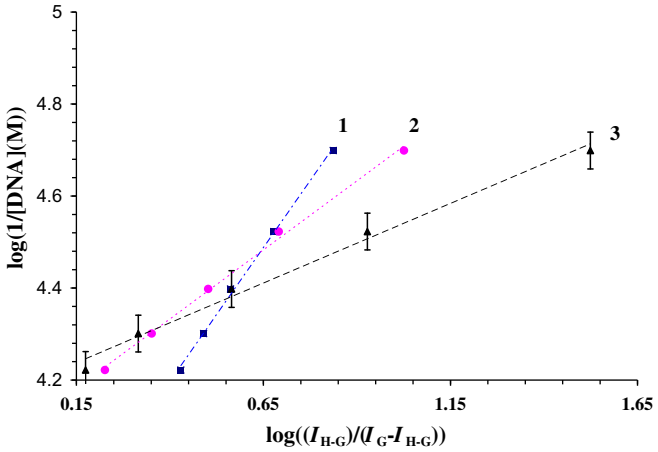

Fig. 4. Plots of log $(I_{H-G}/(I_G - I_{H-G}))$ vs. log(1/[DNA]) used to calculate the binding constants of complexes **1–3** with DNA.

The greater K of these Sn complexes than those observed for similar DNA-intercalating Cr and Ru complexes; $[CrCl_2(dicnq)_2]^+$ and $[Ru((dicnq)_3]^{+2}$, with K reported as 1.20×10^3 and $9.70 \times 10^3\ M^{-1}$ [27–29], suggests their potential candidature as chemotherapeutic agents. The negative values of standard Gibbs free energy ($\Delta G = -RT\ln K$) indicate the spontaneity of their binding interaction with DNA.

For the determination of binding site size the following simple binding model was used [5]:

$$C_b/C_f = K\{[\text{free base pairs}]/s\} \quad (5)$$

where 's' is the binding site size in terms of base pairs. Measuring the concentration of DNA in terms of [NP], the concentration of base pairs can be expressed as [DNA]/2. So Eq. (5) can be written as

$$C_b/C_f = K\{[\text{DNA}]/2s\} \quad (6)$$

C_f and C_b denote the concentrations of free and DNA bound species, respectively.

The C_b/C_f ratio was determined by the equation given below [30]

$$C_b/C_f = (I - I_{DNA})/I_{DNA} \quad (7)$$

where I_{DNA} and I represent the peak current of the drug with and without DNA.

Putting the values of K as calculated according to Eq. (4), the values of binding site size as listed in Table 2 were obtained from the slopes of C_b/C_f versus [DNA] plots. (Fig. 5) The values of 's' decrease in the order: **2** > **3** > **1**. The small binding site size of **1** may be due to its electrostatic interaction with DNA. The results demonstrate that two molecules of complexes **2** and **3** cover one base pair when intercalate into DNA.

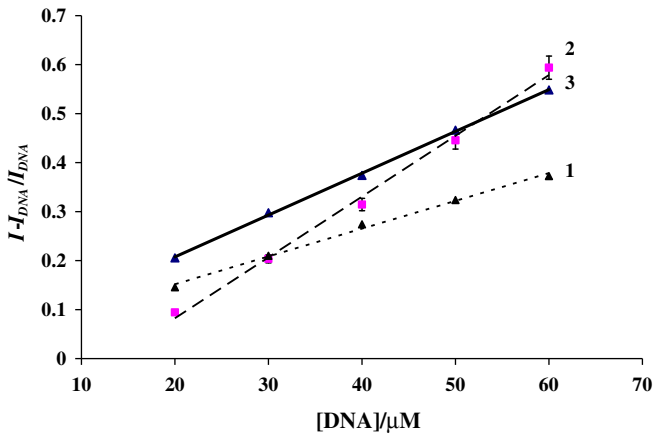

Fig. 5. $I - I_{DNA}/I_{DNA}$ vs. [DNA] for the determination of binding site size.

3.6. UV–Vis spectroscopy

The interaction of complexes **1–3** with DNA was also examined by UV–Vis absorption titration for getting further clues about the mode of interaction and binding strength. The effect of varying

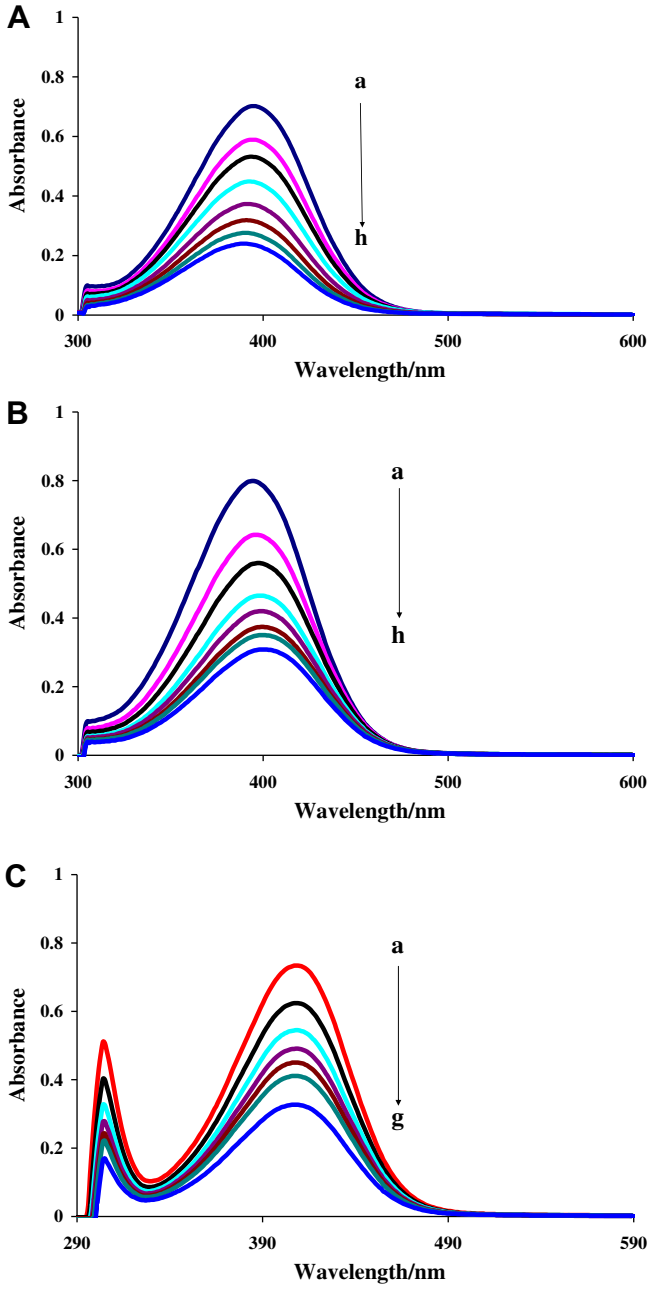

Fig. 6. (A) Absorption spectra of 30 μM **1** in the absence (a) and presence of 20 μM, (b) 30 μM, (c) 40 μM, (d) 50 μM, (e), 60 μM (f), 70 μM (g) and 80 μM DNA (h) in 10% aqueous DMSO at 25 °C. (B) Absorption spectra of 30 μM **2** in the absence (a) and presence of 20 μM, (b) 30 μM, (c) 40 μM, (d) 50 μM, (e), 60 μM (f), 70 μM (g) and 80 μM DNA (h) in 10% aqueous DMSO at 25 °C. (C) Absorption spectra of 30 μM **3** in the absence (a) and presence of 20 μM, (b) 30 μM, (c) 40 μM, (d) 50 μM, (e), 60 μM (f), and 80 μM DNA (g) in 10% aqueous DMSO at 25 °C.

concentration of DNA (20–80 μM) on the electronic absorption spectra of 30 μM **1–3** is shown in Fig. 6A–C. The maximum absorption of complex **1** (Fig. 6A) at λ_{max} = 397 nm, exhibited blue shift of 6 nm, indicating electrostatic interaction of **1** with DNA. Fig. 6B shows that the peak position of 30 μM **2** is shifted bathochromically from λ_{max} = 396 to 403 nm by the addition of 80 μM DNA, accompanied with hypochromic shift from 0.796 to 0.307. These remarkable spectral characteristics suggest intercalation of **2** into the stacked base pairs domain of DNA [31–33]. The hypochromic effect is caused by the overlapping of the electronic states of the intercalating chromophore of the complex **2** with the DNA bases [34] and the bathochromic shift is caused by the lowering in π–π^* transition energy of the complex due to its ordered stacking between the DNA base pairs after intercalation [35]. By the addition of DNA, a slight red shift of peak at 410 nm and pronounce hypochromic effect suggestive of intercalative mode of interaction of **3** (Fig. 6C). In short, UV–Vis results are quite consistent with the CV results.

The binding constants were calculated according to the following Eq. (8) [36–37]:

$$\frac{A_0}{A - A_0} = \frac{\varepsilon_G}{\varepsilon_{H-G} - \varepsilon_G} + \frac{\varepsilon_G}{\varepsilon_{H-G} - \varepsilon_G} \frac{1}{K[DNA]} \quad (8)$$

where K is the binding constant, A_0 and A are absorbance of the free drug and the apparent one, ε_G and ε_{H-G} are their absorption coefficients, respectively.

The slope to intercept ratio of the plot between $A_0/(A - A_0)$ versus 1/[DNA] yielded the binding constant, $K = 1.32 \times 10^3$, 7.21×10^3 and $6.22 \times 10^3\ M^{-1}$ for **1–3**, respectively. The K obtained here follows the same order as was obtained from CV data. The slight difference in the values of UV–Vis and CV binding constant may be due to the use of supporting electrolyte in CV measurements.

4. Conclusions

In summary, new complexes **1–3** of 4-(4-nitrophenyl)piperazine-1-carbodithioate ligand were synthesized and characterized. Spectroscopic exploration confirmed penta-coordinate geometry for **1** and **2**, while hexa-coordinate environment was found around Sn in **3**. The anisobidentate nature of the ligand proposed from the IR spectroscopy concurs well with the reported crystal structures for **1** and **2**. The decrease in peak currents of complexes **1–3**, by the addition of DNA evidenced their interaction with DNA. The positive shift of peak potential in case of **2** and **3** by the addition of DNA, signified the intercalation mode, in which the molecules insert into the base pair domain of DNA, due to which the diffusion coefficients of the bound complexes are lowered as was observed. In general, the diffusion coefficients of the compounds decrease with the increase in molecular weight but the results of our experiments showed opposite trend indicating the dominant role of the ligands in deciding the order in which the D_f values vary. The lower *ks* values of the DNA bound complexes as compared to free complexes indicated slower electron transfer kinetics. The charge transfer coefficient ($\alpha > 0.5$), ratio of peak currents ($I_{pc}/I_{pa} > 1$) and peak potential difference ($\Delta E_p > 60 < 212$) indicated the quasi-reversibility of the redox processes. The binding constant, binding site size and the Gibbs free energy varied in the sequence: **2** > **3** > **1**.

Acknowledgment

The authors are grateful to Higher Education Commission of Pakistan (HEC) for financial support.

References

[1] E.R.T. Tiekink, Appl. Organomet. Chem. 22 (2008) 533.
[2] R.K. Gilpin, Anal. Chem. 69 (1997) 145R.
[3] Y.G. Jun, X.J. Juan, C.H. Yuan, L.Z. Zhou, Chin. J. Chem. 22 (2004) 1325.
[4] M.T. Carter, A.J. Bard, J. Am. Chem. Soc. 109 (1987) 7528.
[5] M.T. Carter, M. Rodriguez, A.J. Bard, J. Am. Chem. 111 (1989) 8901.
[6] T.C. Richards, A.J. Bard, Anal. Chem. 67 (1995) 3140.
[7] M. Rodriguez, A.J. Bard, Anal. Chem. 62 (1990) 2658.
[8] Z. Rehman, S. Shahzadi, S. Ali, G.X. Jin, Turk. J. Chem. 31 (2007) 435.
[9] Z. Rehman, M.M. Barsan, I. Wharf, N. Muhammad, S. Ali, A. Meetsma, Inorg. Chim. Acta 361 (2008) 3322.
[10] Z. Rehman, S. Shahzadi, S. Ali, A. Badshah, J. Iranian Chem. Soc. 3 (2006) 157.
[11] W.F.L. Armarego, C. Chai, Purification of Laboratory Chemicals, 5th ed., Butterworth, Oxford, 2003.
[12] J. Sambrook, E.F. Fritsch, T. Maniatis, Molecular Cloning: A Laboratory Manual, 2nd ed., Cold Spring Harbour Laboratory Press, New York, 1989.
[13] H.D. Yin, S.C. Xue, Appl. Organometal. Chem. 20 (2006) 283.
[14] Z. Rahman, S. Ali, N. Muhammed, A. Meetsma, Acta Crystallogr., Sect. E E63 (2007) m89.
[15] Z. Rahman, S. Ali, N. Muhammad, A. Meetsma, Acta Crystallogr., Sect. E E62 (2006) m3560.
[16] B. Wrackmeyer, Annu. Rep. NMR Spectrosc. 16 (1985) 73.
[17] B. Wrackmeyer, Annu. Rep. NMR Spectrosc. 38 (1999) 203.
[18] A. Tarassoli, T. Sedaghat, B. Neumüller, M. Ghassemzadeh, Inorg. Chim. Acta 318 (2001) 15.
[19] P.G. Harrison, in: P.G. Harrison (Ed.), Chemistry of Tin, 1st ed., Blackie Academic and Professional, London, 1989, p. 105.
[20] X. Jiang, X. Lin, Bioelectrochemistry 68 (2006) 206.
[21] A. Shah, A.M. Khan, R. Qureshi, F.L. Ansari, M.F. Nazar, S.S. Shah, Int. J. Mol. Sci. 9 (2008) 1424.
[22] J.E.B. Randles, Trans. Faraday Soc. 44 (1948) 327.
[23] A. Sevcik, Collect. Czech., Chem. Commun. 13 (1948) 349.
[24] E. Niranjana, R.R. Naik, B.E.K. Swamy, Y.D. Bodke, B.S. Sherigara, H. Jayadevappa, B.V. Badami, Int. J. Electrochem. Sci. 3 (2008) 980.
[25] R.J. Klinger, J.K. Kochi, J. Phys. Chem. 85 (1981) 12.
[26] Q. Feng, N.Q. Li, Y.Y. Jiang, Anal. Chim. Acta 344 (1997) 97.
[27] Q. Lie, P. Yang, H. Wang, M. Guo, J. Inorg. Biochem. 64 (1996) 181.
[28] J. Rusanova, S. Decurtins, E. Rosanov, H.S. Evans, S. Delahaye, A. Hauser, J. Chem. Soc., Dalton. Trans. (2002) 4318.
[29] A. Ambroise, B.G. Maiya, Inorg. Chem. 39 (2000) 4264.
[30] M. Aslanoglu, C.J. Isaac, A. Houlton, B.R. Horrocks, Analyst 125 (2000) 1791.
[31] E.C. Long, J.K. Barton, Acc. Chem. Res. 23 (1990) 273.
[32] G.J. Yang, J.J. Xu, H.Y. Chen, Z.Z. Leng, Chin. J. Chem. 22 (2004) 1325.
[33] L.Z. Zhang, G.Q. Tang, J. Photochem. Photobiol. B: Biol. 74 (2004) 119.
[34] R. Fukuda, S. Takenaka, M. Takagi, J. Chem. Soc., Chem. Commun. 15 (1990) 1028.
[35] X.J. Dang, J. Tong, H.L. Li, J. Inclusion Phenom. 24 (1996) 275.
[36] M.Y. Ni, Y. Wang, H.L. Li, Pol. J. Chem. 71 (1997) 816.
[37] J.B. Lepecq, C. Paoletti, J. Mol. Biol. 27 (1967) 87.